An *arginase 2* promoter transgenic illuminates anti-inflammatory signalling in zebrafish

Ffion R. Hammond[1]*, Amy Lewis[1]*, Holly E. Anderson[1], Lewis G. Williams[1], Annemarie H. Meijer[2], Geert F. Wiegertjes[3] and Philip M. Elks[1]

[1]The Bateson Centre, Department of Infection and Immunity and Cardiovascular Disease, University of Sheffield, Western Bank, Sheffield, UK.

[2]Institute of Biology Leiden, Leiden University, Einsteinweg 55, 2333 CC, Leiden, The Netherlands.

[3]Aquaculture and Fisheries Group, Department of Animal Sciences, Wageningen University & Research, 6700 AH Wageningen, The Netherlands.

* These authors contributed equally.

Corresponding author:

Dr Philip M. Elks

The Bateson Centre,

University of Sheffield,

Firth Court,

Western Bank,

Sheffield,

South Yorkshire,

S10 2TN.

UK

Tel: +44 (0) 1142 223609

p.elks@sheffield.ac.uk

Abstract

The innate immune response to inflammatory stimuli must be finely balanced to produce an appropriate pro-inflammatory response while allowing a subsequent return to homeostasis. In recent years, *in vivo* transgenic zebrafish models have shed light on the temporal regulation of the pro-inflammatory innate response to immune challenges. However, until now, there have been no zebrafish transgenic models of anti-inflammatory signalling. We compared existing expression data of arginase genes in zebrafish neutrophils and macrophages, strong candidates for an anti-inflammatory marker, and identified that *arginase 2* is the most highly expressed Arginase in zebrafish immune cells. We developed an *arginase 2* (*arg2*) bacterial artificial chromosome (BAC) transgenic line, *TgBAC(arg2:eGFP)sh571*, driving GFP expression under the control of the *arg2* promoter. We show that, under resting conditions, *arg2:GFP* is expressed in ionocytes, matching the *in situ* hybridisation pattern. Upon immune challenge by injury, bacterial and fungal insults, *arg2:GFP* is predominantly expressed in neutrophils at early timepoints post-insult. Later in infections, *arg2:GFP* is expressed in cells associated with foci of infection (including neutrophils and macrophages), alongside liver expression. Our data indicate that *arginase 2* is predominantly expressed in neutrophils after immune challenge and suggest that anti-inflammatory signals coincide with pro-inflammatory signals during early wound and infection responses.

Introduction

Initial immune responses to inflammatory or infection stimuli are mediated by innate immune cells, of which leukocytes are major players. Two important leukocyte cell types, neutrophils and macrophages, work together to neutralise invading threats whilst promoting tissue healing and restoration of homeostasis. Neutrophils and macrophages have evolved together and co-exist in invertebrate and vertebrate species [1]. Neutrophils are often observed to be the first immune cell type to respond to immune challenge, rapidly migrating towards the stimuli and becoming activated to a pro-inflammatory and antimicrobial state,

clearing damaged cells and invading pathogens. Macrophages also rapidly respond to challenge, with pro-inflammatory phenotypes emerging soon after immune challenge aiding microbial clearance (often termed M1 or classical activation). Dogmatically, neutrophils are considered a blunt first line of defense that once activated remain so until cleared from tissues, either by apoptosis and subsequent efferocytosis by macrophages or by migration away [2–4]. Persistence of neutrophils during disease can cause considerable bystander damage to healthy surrounding tissues driving chronic pathologies. Macrophage phenotypes, on the other hand, are well-characterised as being plastic throughout the pathogenesis of inflammation and infections in a process termed macrophage polarisation. Pro-inflammatory macrophage phenotypes are followed by anti-inflammatory phenotypes that promote healing and restoration of homeostasis (often termed M2 or alternatively activated). Many of the above observations come from *in vitro* approaches. *In vivo* exploration indicates that macrophage polarisation is not binary but rather a spectrum of phenotypes and behaviours, and that the neutrophil response is more plastic than previously thought, with emerging roles for neutrophil subsets in tissue protection and healing [5–7].

Both neutrophils and macrophages are activated by danger and pathogen associated molecular patterns (DAMPs and PAMPs), which trigger the production of pro-inflammatory signals (e.g. IL-1β and TNF-α) after immune challenge [8,9]. These activate the production of antimicrobial molecules, including reactive nitrogen species (RNS), via the enzyme inducible nitric oxide synthase (iNOS) [10]. Immunomodulatory signals are required to limit and eventually turn-off the pro-inflammatory response in order for tissues to regain homeostasis. The best characterised of these anti-inflammatory signaling molecules are cytokines including the interleukins (IL), IL-4, IL-13 and IL-10, alongside proteins that dampen the pro-inflammatory response, including Arginase [11]. Despite their classification as anti-inflammatory, these signals have also been identified as being upregulated in some pro-inflammatory situations [12]. The production of antimicrobial RNS is negatively regulated by the enzyme Arginase. Arginase competes with iNOS for a shared substrate, L-arginine, a

limited resource within the cell. The immunomodulatory properties of Arginase extend beyond the regulation of RNS production. Arginase 2 is essential for IL-10 mediated downregulation of pro-inflammatory factors making it a key anti-inflammatory enzyme [13]. Arginase and iNOS have been well-characterised in murine models as being strongly expressed in macrophage subtypes, with Arginase being a wound-healing/anti-inflammatory macrophage marker and iNOS a pro-inflammatory macrophage marker [14]. In human macrophages the distinction between iNOS and Arginase expressing macrophage subtypes is less well-defined, due, in part, to lower macrophage RNS in humans compared to mice. Interestingly, human neutrophils constitutively express Arginase with levels increasing after infection *in vitro*, but its roles are poorly understood *in vivo* [15]. Considering that Arginase is not expressed highly by murine neutrophils [16,17], alternative *in vivo* models are required to investigate the roles of Arginase in immunomodulation and human disease.

The zebrafish has become a powerful model organism to determine the molecular mediators of immunity against injury and pathogenic challenges [18,19]. Advantages of the zebrafish model include transparent larvae combined with fluorescent transgenic lines, allowing detailed microscopy in an intact organism *in vivo*. A key turning-point in zebrafish immunity research came with the development of transgenic lines marking neutrophil and macrophage cell populations. Initially, transgenic lines were developed that labelled whole populations of immune cells in zebrafish larvae, e.g., *TgBAC(mpx:GFP)i114* labelling the total neutrophil population and *Tg(mpeg1:GFP)* labelling the total macrophage population [20,21]. More recently, transgenic lines of important pro-inflammatory cytokines have become available (e.g., *TgBAC(tnfa:GFP)pd1028* and *TgBAC(il-1beta)sh445*)) allowing in-depth analysis of the cells producing these important signals following a variety of immune challenges *in vivo* [22,23]. These transgenic lines utilised bacterial artificial chromosome (BAC) technology, that allows tens of kilobases of promoter region to be used to drive the fluorescent protein, ensuring that the expression of the transgene recapitulates endogenous expression patterns as closely as possible. A key gap in this zebrafish “transgenic toolbox” is an anti-inflammatory fluorescent transgenic line. We therefore set out to develop an *arginase*

2 promoter driven BAC transgenic line to understand the *arginase* response to immune challenge *in vivo*.

Here, we compared existing expression data of *arginase* genes in zebrafish neutrophils and macrophages and show that *arg2* is the most highly expressed *arginase* in zebrafish immune cells. We developed a new BAC transgenic line that drives GFP under the control of the *arginase 2* promoter and demonstrate that the *arg2:GFP* transgene is expressed in ionocytes, a population of skin resident cells, in resting conditions. Following a range of immune challenges, including tailfin transection (sterile injury), *Mycobacterium marinum* (bacterial), and *Cryptococcus neoformans*/*Candida albicans* (fungal) infections, *arg2:GFP* was predominantly upregulated in neutrophils. We identify a small population of macrophages that express *arginase 2* after injury and infection suggesting the presence of anti-inflammatory macrophages in zebrafish. The *arg2:GFP* transgenic line has the potential to uncover new mechanisms behind innate immune regulation during *in vivo* immune challenge.

Materials and Methods

Ethics statement and zebrafish

All zebrafish were raised in the Biological Services Unit (BSU) aquarium (University of Sheffield, UK) and maintained according to standard protocols (zfin.org) in Home Office approved facilities. All procedures were performed on embryos less than 5.2 dpf (days post fertilisation) which were therefore outside of the Animals (Scientific Procedures) Act, to standards set by the UK Home Office. Adult fish were maintained at 28°C with a 14/10 hour light/dark cycle. To investigate expression in immune cells the *TgBAC(arg2:eGFP)sh571* (hereon in termed *arg2:GFP*) reporter line was crossed with the macrophage reporter *Tg(mpeg1:mCherryCAAX)sh378* [24] (hereon in termed *mpeg:mCherry*) and the neutrophil reporter *Tg(lyz:nfsB.mCherry)sh260* [25] (hereon in termed *lyz:mCherry*) to generate embryos for experiments.

140

141 **Generation of *TgBAC(arg2:eGFP)sh571* transgenic zebrafish**

142 An eGFP SV40 polyadenylation cassette was inserted at the *arg2* ATG start site of
143 the zebrafish bacterial artificial chromosome (BAC) CH-211-12d10 using established
144 protocols [21]. Inverted Tol2 elements were inserted into the chloramphenicol coding
145 sequence and the resulting modified BAC containing 115130 base pairs of the *arg2*
146 promoter region was used. We identified two founder zebrafish (allele codes sh571 and
147 sh572) and raised colonies. The embryos of both alleles had the same GFP expression
148 pattern. The data generated in this manuscript is from the *TgBAC(arg2:eGFP)sh571*
149 transgenic line (hereon in termed *arg2:GFP*) as this line had a higher fecundity than
150 *TgBAC(arg2:eGFP)sh572*.

151

152 **Tailfin transection**

153 To induce an inflammatory stimulus, 2- or 3-days post fertilisation (dpf) zebrafish
154 were anaesthetised in 0.168 mg/ml Tricaine (Sigma-Aldrich) in E3 media and visualised
155 under a dissecting microscope. Using a scalpel blade (5mm depth, WPI) the tailfin was
156 transected after the circulatory loop as previously described ensuring the circulation
157 remained intact [26].

158

159 **Pathogen strains and culture**

160 Bacterial infection experiments were performed using *Mycobacterium marinum* strain
161 M (ATCC #BAA-535), containing the pSMT3-Crimson vector, with liquid cultures prepared
162 from bacterial plates [27]. Liquid cultures were washed and prepared in 2%
163 polyvinylpyrrolidone40 (PVP40) solution as previously described for injection [28,29].
164 Injection inoculum was prepared to 100 colony forming units (cfu)/nl for all *Mm* experiments,
165 which was injected into the circulation at 30hpf via the caudal vein.

166 Fungal infection experiments were performed using the *Candida albicans* strain
167 TT21-*mCherry* [30]. Overnight liquid cultures were grown from fungal plates, then prepared

for injection as previously described [30]. Cultures were counted using a hemocytometer and prepared in 10% PVP40 for 200cfu/nl injection dose which was injected into the circulation at 30hpf via the caudal vein.

Fungal infection experiments were also performed using the *Cryptococcus neoformans* strain Kn99-*mCherry* [31]. Cryptococcal culture was performed as previously described [24] and after counting on a hemocytometer, Kn99 was prepared in 10% PVP40 for 200cfu/nl injection dose which was injected into the circulation at 1-2dpf.

Microinjection of zebrafish larvae

Prior to injection, zebrafish were anaesthetised in 0.168 mg/ml Tricaine (MS-222, Sigma-Aldrich) in E3 media and transferred onto 1% agarose in E3+methylene blue plates, removing excess media. All pathogens were injected into the circulation to create systemic infection, using a microinjection rig (WPI) attached to a dissecting microscope. A 10mm graticule was used to measure 1nl droplets for consistency, and droplets were tested every 5-10 fish and recalibrated if necessary. Final injection volume of 1nl was injected to produce doses calculated for each pathogen. After injection, zebrafish were transferred to fresh E3 media for recovery and maintained at 28°C.

Whole mount *in situ* hybridisation

RNA probes for zebrafish arginase type II (*arg2*, ENSDARG00000039269. Plasmid obtained from Source Bioscience) were designed and synthesised after cloning into the pCR™Blunt II-TOPO® vector according to manufacturer's instructions (ThermoFisher Scientific). Plasmids were linearised and probes synthesised according to DIG RNA Labeling Kit (SP6/T7) (Roche). Zebrafish larvae were fixed in 4% paraformaldehyde solution (PFA, ThermoFisher Scientific) overnight at 4°C. Whole mount *in situ* hybridisation was performed as previously described [32].

Confocal microscopy

196 Control, tailfin transected, and infected larvae were imaged using a Leica DMi8 SPE-
197 TCS microscope using a HCX PL APO 40x/1,10 water immersion lens. For confocal
198 microscopy larvae were anaesthetised in 0.168 mg/ml Tricaine and mounted in 1% low
199 melting agarose (Sigma) containing 0.168 mg/ml tricaine (Sigma) in 15µ-Slide 4 well glass
200 bottom slides (Ibidi).
201
202 **Stereo microscopy**
203 Zebrafish larvae were anaesthetised in 0.168 mg/ml Tricaine and transferred to a
204 50mm glass bottomed FluoroDish™ (Ibidi). Zebrafish were imaged using a Leica DMi8 SPE-
205 TCS microscope fitted with a Hamamatsu ORCA Flash 4.0 camera attachment using a HC
206 FL PLAN 2.5x/0.07 and HC PLAN APO 20x/0.70 dry lens. Both transgenic zebrafish and
207 whole mount *in situ* staining was imaged using a Leica MZ10F stereo microscope fitted with
208 a GXCAM-U3 series 5MP camera (GT Vision).
209
210 **Lightsheet microscopy**
211 2 and 3dpf larvae were imaged using a Zeiss Z1 lightsheet microscope with Plan-
212 Apochromat 20x/1.0 Corr nd=1.38 objective, dual-side illumination with online fusion and
213 activated Pivot Scan at 28°C chamber incubation. Zebrafish were anaesthetised in 0.168
214 mg/ml Tricaine and mounted vertically in 1% low melting agarose (Sigma) in a glass
215 capillary. Images were obtained using 16bit image depth, 1400x1400 pixel field of view and
216 GFP visualised with 488nm laser at 16% power, 49.94ms exposure and user-defined z-stack
217 depth (400-600 slices, 0.641µm slices).
218
219 **Data analysis**
220 Microscopy data was analysed using Leica LASX (Leica Microsystems) and Image J
221 software. Graphs were generated using Prism 8.0, GraphPad Software (San Diego, CA,
222 USA).
223

Results

TgBAC(arg2:GFP)sh571 is expressed in ionocytes in resting conditions

There are two isozymes of Arginase in most mammals and fish, Arginase 1 (ARG1) and Arginase 2 (ARG2). In mice, ARG1 and ARG2 are both expressed by macrophages, however it is ARG1 that is the most widely studied in macrophage polarisation, with increased expression of cytosolic ARG1 protein depleting intracellular stores of arginine [33]. In fish, Arginases have been studied in common carp (*Cyprinus carpio*), a species phylogenetically close to zebrafish, where *arg2* is the most highly expressed of the Arginase family in immune cells [11,34]. Head-kidney derived macrophages of carp which have been polarised towards anti-inflammatory phenotypes using cAMP have a 16-fold upregulation of *arg2* expression [11,35].

Zebrafish have orthologues of mammalian Arginase 1 and Arginase 2, which were compared using existing transcriptomics datasets to identify innate immune cell expression. FACS purified neutrophils (*Tg(mpx:GFP)i114*) and macrophages (*Tg(mpeg1:Gal4-VP16)gl24/(UAS-E1b:Kaede)s1999t*) from unchallenged 5dpf larvae both expressed *arginase2* (*arg2*), while *arginase 1* (*arg1*) was not expressed at detectable levels (Supplemental Figure 1A-B, using raw data from [36]). *arg2* expression was found at high levels in the bulk, non-immune cell, population alongside being expressed in the immune cell populations (Supplemental Figure 1C-D, data from [36]). *arg2* expression was approximately 1.5-fold higher in neutrophils than macrophages in unchallenged zebrafish larvae (Supplemental Figure 1C-D, using raw data from [36]). In unchallenged adult zebrafish, single-cell RNAseq identified *arg2* expression in a population of neutrophils, a smaller population of monocytes/macrophages, with no detectable expression in other blood lineages (thrombocytes/erythrocytes) (Supplemental Figure 1E-F, data from The Zebrafish Blood Atlas, https://www.sanger.ac.uk/science/tools/basicz/basicz/, [37]). From the same dataset *arg1* was not detected in any immune cell lineage (Supplemental Figure 1E-F).

Based on the predominant expression of *arg2* in fish innate immune cells, we chose to develop an *arg2* transgenic zebrafish line to investigate its expression during immune challenge *in vivo*. We adopted a BAC transgenesis approach, using a BAC (CH-211-12d10) in which 11.5kb of the *arg2* promoter drives GFP expression, to generate two transgenic line alleles with the same expression (*TgBAC(arg2:eGFP)sh571* and *TgBAC(arg2:eGFP)sh572*). Due to the higher fecundity in the *sh571*, it was this line that was used in the following studies (hereon in termed *arg2:GFP*).

In unchallenged *arg2:GFP* larvae, the transgene was expressed in cuboidal-shaped cells in the skin, distributed over the yolk and caudal vein regions at 2 days post fertilisation (dpf, Figure 1A) and 3dpf (Figure 1B-C). A subset of ionocytes, cells in the skin responsible for the transport of sodium ions also known as H^+-ATPase-rich cells (HRCs), have been shown to express high levels of *arginase 2* by *in situ* hybridisation in zebrafish [38–40]. *arg2:GFP* expression recapitulated the *arginase 2 in situ* hybridisation pattern, labelling ionocytes (Figure 1D-E). To determine whether any of the cells over the yolk area expressing *arg2:GFP* were leukocytes, we crossed the *arg2:GFP* line with a macrophage transgenic line (*Tg(mpeg1:mCherry)sh378*, hereon in termed *mpeg:mCherry*) and a neutrophil transgenic line (*Tg(lyz:nsfB.mCherry)sh260*, hereon in termed *lyz:mCherry*). Under resting conditions there was no overlap between *mpeg:mCherry* positive macrophages and *arg2:GFP* positive cells at 2dpf, 3dpf, 4dpf or 5dpf (Figure 1F-G). Nor was there overlap between *lyz:mCherry* positive neutrophils (Figure 1H). These data indicate that the *arg2:GFP* line is not expressed at detectable levels in immune cells in resting conditions at these developmental timepoints, matching *in situ* hybridisation data. The zebrafish *arg2:GFP* transgene and *in situ* hybridisation did not detect leukocyte *arginase 2* expression in resting conditions, however *arginase 2* levels were detected by RNAseq of FACS purified leukocyte populations (Supplemental Figure 1). This suggests that either the transgenic and *in situ* hybridisation techniques were not as sensitive as RNAseq, or that techniques to purify immune cells in RNAseq studies have led to upregulation of *arg2* not present in the intact zebrafish.

279

280 ***arg2:GFP* is predominantly upregulated by neutrophils after tailfin transection**

281 To assess whether *arg2:GFP* expression is upregulated in innate immune cells
282 during an immune response, we challenged 2dpf larvae with a sterile tailfin wound. Using a
283 tailfin nick model we identified that highly mobile immune cells migrating towards the wound
284 expressed *arg2:GFP* within the first hour of timelapse microscopy (Figure 2A). We reasoned
285 that these cells were neutrophils, due to their size and amoeboid shape alongside their rapid
286 migration towards the wound. To investigate whether neutrophils expressed *arg2:GFP* after
287 injury, we crossed the *arg2:GFP* line with the neutrophil *lyz:mCherry* transgenic line.
288 Timelapse microscopy demonstrated that a subpopulation of neutrophils arriving at the tailfin
289 transection wound were *arg2:GFP* positive by 1 hour post wound (hpw) (Figure 2B) with
290 positive neutrophils at the site of injury present during the recruitment phase of inflammation
291 (1-6hpw) while expression was not observable in neutrophils away from the wound. There
292 was no expression of *arg2:GFP* observed in *mpeg:mCherry* positive macrophages in the
293 recruitment phase of inflammation between 1-6hpw (Figure 2C).

294 In order to observe potential anti-inflammatory macrophages, *mpeg:mCherry* larvae
295 crossed into the *arg2:GFP* line were imaged at a later timepoint, 3dpw (5dpf), by which time
296 the fin has partially regenerated. In uninjured larvae there were few *mpeg:mCherry* positive
297 macrophages in the tailfin fold at 5dpf and these did not express *arg2:GFP* (Figure 2D, top
298 panel). In tailfin transected larvae there were increased numbers of macrophages in the
299 2dpw and 3dpw healing/regenerating tailfin fold, but the majority of these were *arg2:GFP*
300 negative, while *mpeg:mCherry* negative cells with the morphology of neutrophils did express
301 *arg2:GFP* (Figure 2D, bottom two panels). Upon closer investigation using confocal
302 microscopy, *mpeg:mCherry* positive cells expressing *arg2:GFP* were identified at the wound
303 at 2dpw and 3dpw (Figure 2E), though these were greatly outnumbered by *arg2:GFP*
304 negative macrophages. *arg2:GFP* positive macrophages were not observed in uninjured
305 larvae. Together these data hint at the presence of *arginase 2* expressing anti-inflammatory
306 macrophages during tailfin regeneration.

307

308 **Infection challenge upregulates neutrophil *arg2:GFP* expression**

309 To investigate the expression of *arg2* after bacterial infection, *arg2:GFP* embryos
310 were injected with *Mycobacterium marinum* (Mm) at 1dpf. We assessed the early response
311 to Mm infection at 1dpi and found that a subpopulation of neutrophils express *arg2:GFP*
312 early in infection (Figure 3A). Neutrophil *arg2:GFP* expression was not observed in mock-
313 infected (PVP) controls (Figure 3B) with ionocyte expression confirming *arg2:GFP* positive
314 larvae. *arg2:GFP* positive neutrophils were present in the vicinity of Mm infection (Figure
315 3A), with both infected and uninfected neutrophils expressing *arg2:GFP* (Figure 3C). A
316 subset of neutrophils had *arg2:GFP* expression, with 31.7% (of n=123 neutrophils) of
317 *lyz:mCherry* positive neutrophils in the region of infection expressing GFP, suggestive of
318 differential immune responses between individual neutrophils (Figure 3D-E). At the same
319 1dpi timepoint, 6.1% (of n=98 macrophages) of *mpeg:mCherry* positive macrophages were
320 positive for *arg2:GFP* (Figure 3E-G).

321 Fungal infections have been shown to modulate host arginine metabolism via
322 Arginase [41], therefore we assessed *arg2:GFP* expression in two well-characterised fungal
323 zebrafish infection models - *Candida albicans* [42] and *Cryptococcus neoformans* [24]. In
324 both fungal infections, *arg2:GFP* was observed in a subpopulation of *lyz:mCherry* positive
325 neutrophils at 1dpi (Figure 4A-B). As with Mm infection, subsets of neutrophils both with or
326 without internalised pathogen were *arg2:GFP* positive in *Candida albicans* infection (Figure
327 4A). *arg2:GFP* positive *mpeg:mCherry* macrophages were also observed in *Cryptococcus*
328 *neoformans* infection at 1dpi, however these were greatly outnumbered by negative
329 macrophages and only 3 examples were identified (Supplemental Figure 2). In Cryptococcal
330 infected larvae with a high fungal burden, *arg2:GFP* expression was observed in the liver
331 (Figure 4C-D) at timepoints when this was not present in PVP injected larvae (Figure 4C).
332 This was especially apparent in Cryptococcus infections at 2dpi (Figure 4D) and was
333 confirmed by *in situ* hybridisation (Figure 4E). Arginase is a well characterised liver enzyme
334 [43], yet in unchallenged embryos (Figure 1A-E) or PVP injected larvae (Figure 4C) there

was no visible liver expression of *arg2:GFP*. Liver expression was also present after Mm infection, but was less pronounced (Supplemental Figure 3). Like Cryptococcal infected larvae this occurred in individuals highly infected with Mm, but was not observed till later in infection (at 4dpi), potentially reflecting the slower doubling time/pathogenesis of Mm compared to Cryptococcus.

arg2:GFP is expressed in cells associated with developing granulomas

arg2:GFP expression was assessed at a later stage of Mm infection (4dpi), a stage at which innate immune granulomas are forming and when it is likely that leukocyte phenotypes are more diverse and polarised due to immune modulation by mycobacteria [44]. PVP control injected larvae had minimal *arg2:GFP* expression, apart from ionocyte expression and background green signal from the autofluorescence of pigment cells (Figure 5A). In Mm infected larvae, *arg2:GFP* was expressed in cells associated with developing granulomas at 4dpi (Figure 5B). The brightest population of these cells were *lyz:mCherry* positive, indicating a subset of *arg2:GFP* positive granuloma-associated neutrophils, representing 37.5% of neutrophils imaged in granulomas (Figure 5C-E). There were also granuloma-associated *arg2:GFP* expressing cells that were *lyz:mCherry* negative (Figure 5C), some containing phagocytosed bacteria (Figure 5C and F) and expressing macrophage *mpeg:mCherry* (Figure 5F). *mpeg:mCherry* positive macrophages had lower *arg2:GFP* expression in comparison to the *mpeg:mCherry* negative/*arg2:GFP* positive granuloma-associated cells (Figure 5F-H). *arg2:GFP* expression was observed in both infected and non-infected *mpeg:mCherry* positive macrophages (Figure 5F-H). Due to the dim and variable expression of both *arg2:GFP* and *mpeg:mCherry*, numbers of positive granuloma-associated macrophages were difficult to accurately quantitate, but *arg2:GFP* positive *mpeg:mCherry* macrophages were outnumbered by *arg2:GFP* negative *mpeg:mCherry* macrophages and *arg2:GFP* positive *lyz:mCherry* neutrophils in granulomas. Together, these data suggest that Mm granulomas have *arginase* expressing neutrophils and that

362 other granuloma-associated cells, including potential anti-inflammatory macrophages, also
363 express *arginase*.
364
365 **Discussion**
366 Zebrafish transgenic lines have allowed *in vivo* exploration of the pro-inflammatory
367 immune response (including *il-1β* and *tnfa*) to a variety of stimuli, however, until now, there
368 has been a lack of similar tools for anti-inflammatory factors [22,23,45]. Here, we describe a
369 new transgenic line for *arginase 2* and show that this transgene is upregulated shortly after
370 immune challenge in neutrophils and a small subset of macrophages. These data correlate
371 with a growing body of evidence that suggest anti-inflammatory factors are expressed early
372 after immune challenge to suppress hyper-inflammation before a switch to an anti-
373 inflammatory environment is required at later stages for tissue healing and restoration of
374 homeostasis [46].
375 The *arg2:GFP* line shows that neutrophils are the predominant immune cell type that
376 express *arginase 2* early after immune challenge in zebrafish. The observation of *arginase 2*
377 expression in zebrafish neutrophils fits with our previous observations that zebrafish
378 neutrophils are the primary innate immune cell that produce antimicrobial reactive nitrogen
379 species (RNS) after Mm infection and suggests a neutrophil iNOS/Arginase balance [47].
380 Human neutrophils also produce high levels of RNS [12], differing from expression in mice
381 where it is primarily macrophages that produce RNS/Arginase [12,16,48,49]. Human
382 polymorphonuclear neutrophils (PMNs) produce high levels of Arginase at a transcript and
383 protein level following immune challenge and in resting states, that may act as a negative
384 regulator of the RNS response, as is the case in murine macrophages. [12,16,48,49].
385 The mechanisms balancing innate immune regulation during inflammatory and
386 infection responses are not well understood *in vivo*. Neutrophil *arg2:GFP* was observed at
387 timepoints that are considered to be pro-inflammatory stages of inflammation and infection.
388 *arg2:GFP* expression was reminiscent of our previous observations using the pro-

389 inflammatory *TgBAC(il-1 β:GFP)sh445* transgenic line, where neutrophil *il-1β* was found at
390 1hpw in the tailfin and 1dpi in Mm infections, the same timepoints that *arg2:GFP* was
391 observed [23]. This suggests that anti-inflammatory *arginase* expression coincides with pro-
392 inflammatory signals in neutrophils, evidence for a balanced response. The observation of
393 immune cells producing anti-inflammatory signals upon immune challenge has been
394 observed previously, but to date this has been mainly described in macrophages [46]. It is
395 becoming clear that a balanced response to immune challenge, including both pro- and anti-
396 inflammatory signals is beneficial in disease control [46]. In murine macrophages it has been
397 demonstrated *in vitro* that Arginase 1 is produced soon after infection and can have
398 immunomodulatory effects [16]. Our findings open up the possibility that a similar balance
399 may exist in neutrophils and add to recent evidence suggesting that neutrophil phenotypes
400 are more diverse and nuanced than previously appreciated [6,7].

401 Some pathogens have evolved to disrupt the pro- and anti-inflammatory response,
402 keeping pro-inflammatory factors low and increasing anti-inflammatory signals to allow for
403 immune cell evasion and survival. One such pathogen is *Mycobacterium tuberculosis* (Mtb),
404 that suppresses an initial pro-inflammatory response, in part by upregulation of macrophage
405 Arginase, to allow for intra-phagocyte survival and intracellular growth and proliferation to
406 form hallmark granuloma structures [16]. This makes Arginase a potential target for
407 therapeutic intervention during TB. In murine TB models, macrophage Arginase expression
408 is associated with decreased bacterial killing and is an immunomodulatory target of
409 *Mycobacterium tuberculosis* [16]. Similar observations have been described in fungal
410 infections, with mice infected with Cryptococcus (*Cryptococcus gattii*) having elevated levels
411 of Arginase expression in lung tissues [50]. In human-monocyte-derived macrophages,
412 *Candida albicans* infection induces Arginase that blocks host NO production as a fungal
413 survival mechanism via chitin exposure [41]. Our findings using the *arg2:GFP* line are
414 consistent with these mammalian observations, with early *arginase* expression observed in
415 innate immune cells after Mm and fungal infection. Further investigation is required to
416 understand the molecular mechanisms of this intriguing host-pathogen interaction.

417 Arginase has been described as an anti-inflammatory macrophage marker due, in
418 part, to high expression levels observed in mouse monocytes cultured with anti-inflammatory
419 stimuli such as IL-4 or IL-13 to make M2/anti-inflammatory macrophages and observations
420 in other murine macrophage models [51]. We observed macrophages expressing *arg2:GFP*
421 during infection and at wound-healing stages of tailfin transection. Our findings complement
422 studies on a zebrafish pro-inflammatory macrophage *tnfa* transgenic line, which suggest that
423 an anti-inflammatory population of macrophages exist based on the switching off of *tnfa:GFP*
424 in some macrophages during the wound-healing phase of tailfin transection, and are
425 consistent with anti-inflammatory macrophages being present in the developing zebrafish
426 larvae [45]. However in both inflammation and infection, *arginase*-expressing macrophages
427 were much less frequent than *arginase*-expressing neutrophils, and neutrophil *arginase*
428 expression predominated. It is important to note that the *mpeg1* promoter used to mark
429 macrophages in our study is downregulated by Mm infection [52] therefore it is possible that
430 our observations using the *mpeg1:mCherry* line is an underestimation of the population of
431 macrophages that express *arg2:GFP* during Mm infection. This seems likely as there are
432 many *arg2:GFP* positive granuloma-associated cells, some with phagocytosed bacteria, that
433 expressed *arg2:GFP* but were neutrophil-marker negative, indicative of macrophages that
434 lack visible *mpeg1:mCherry* marker. The granuloma-associated *arg2:GFP* observed may
435 also be expressed in epithelioid-like cells that make up a large proportion of the zebrafish
436 Mm granuloma structure, some of which are macrophage derived but may have lost
437 macrophage markers [44]. Here, we have identified *mpeg1:mCherry* positive granuloma
438 associated macrophages that express *arginase 2*, however it remains unclear as to how
439 many macrophages are polarised towards this potential anti-inflammatory phenotype in
440 zebrafish. Characterising the macrophage polarisation infection response fully will require
441 further study for which the *arg2:GFP* zebrafish line will be an important tool.

442 Outside of immune cells, the *arg2:GFP* line has also illuminated arginase expression
443 in the liver in highly infected individuals and in ionocytes, during both resting and
444 inflammatory states. Arginase is a well-characterised liver enzyme [53,54] therefore

445 expression here was not unexpected, though the function of the upregulated liver expression
446 in highly infected individuals remains unclear. Interestingly, ionocytes have recently been
447 described as a new airway epithelial cell type in human and mice and it is these cells that
448 most highly express cystic fibrosis transmembrane conductance regulator (CFTR) the anion
449 channel that is mutated in cystic fibrosis patients [55]. The *arg:GFP* line is a new tool that
450 could be used to investigate the roles of these intriguing cells *in vivo*.

451 Our data indicate that *arginase 2*, an important anti-inflammatory mediator, is
452 produced early after immune challenge, predominantly by neutrophils. The *arg2:GFP* line is
453 an exciting addition to the zebrafish transgenic toolbox with which to investigate innate
454 immunity during infections. It has the potential to be applied to multiple zebrafish disease
455 models of infection and inflammation and may also be relevant to any models with an
456 inflammatory component, from ageing to cancer.

457

458 **Figures and legends**

459

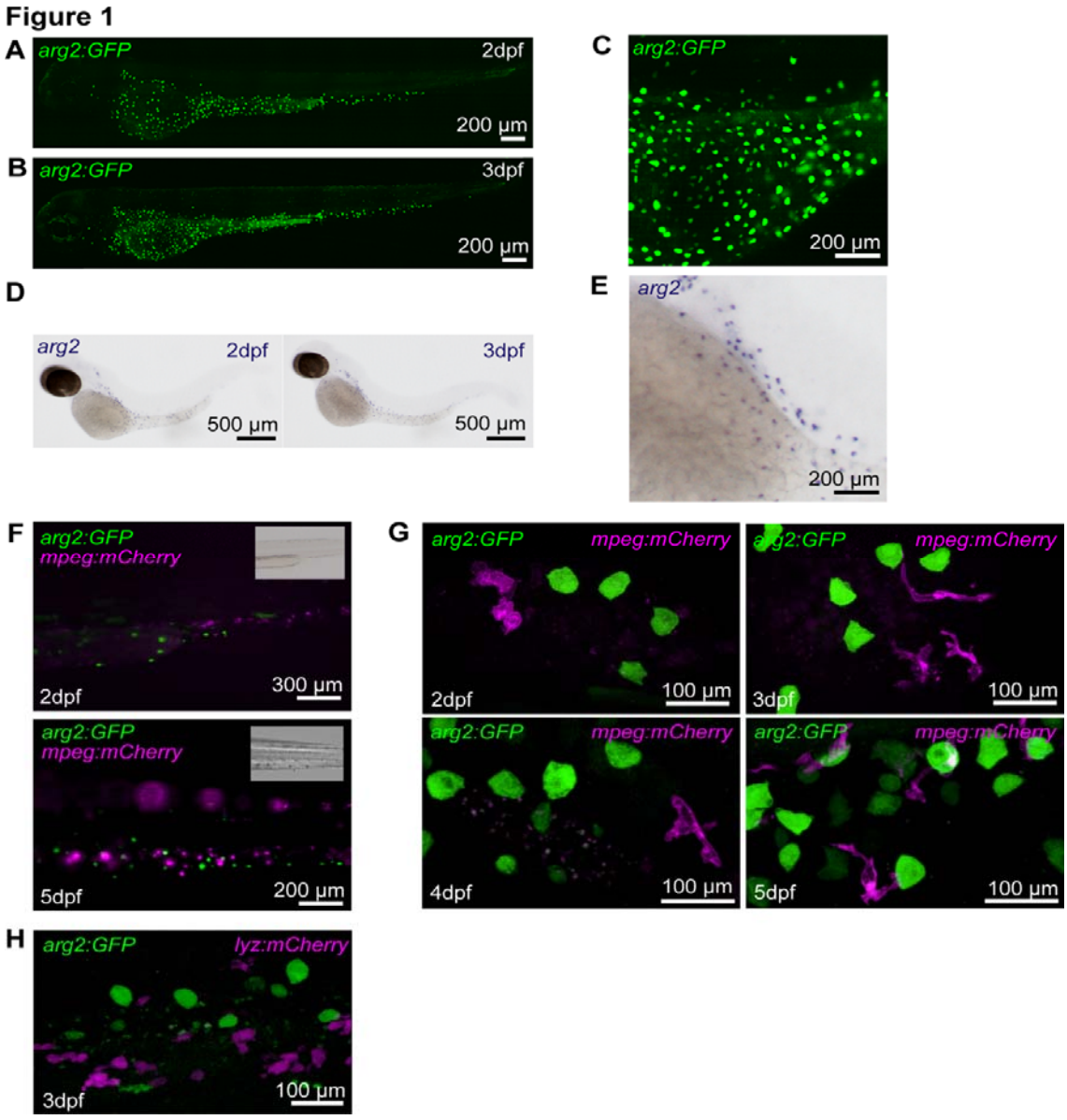

460

461 **Figure 1: The *TgBAC(arg2:eGFP)sh571* line shows GFP expression in ionocytes but**
462 **not in resting macrophages and neutrophils, recapitulating the *arginase 2 in situ***
463 **hybridisation expression pattern**

464 (A-B) Lightsheet microscopy stereo micrographs of *TgBAC(arg2:eGFP)sh571* line shows
465 ionocytes expression at 2 (A) and 3dpf (B).

466 (C) Enlarged image of section over yolk of (B).

(D) *arginase 2 in situ* hybridisation shows expression in cells over the yolk known as ionocytes at 2 and 3 dpf in unchallenged zebrafish.

(E) Enlarged image of section over yolk of 3dpf larvae in (D).

(F) Stereo fluorescence micrographs of *arg2:GFP* crossed to *Tg(mpeg1:mCherry)sh378* at 2dpf and 5dpf with no overlap of *arg2:GFP* expression in ionocytes with magenta macrophages.

(G) Stereo fluorescence micrograph of *arg2:GFP* crossed to *Tg(mpeg1:mCherry)sh378* at 2dpf, 3dpf, 4dpf and 5dpf with no overlap of *arg2:GFP* expression in ionocytes with magenta macrophages.

(H) Stereo fluorescence micrograph of *arg2:GFP* crossed to *Tg(lyz:nfsB.mCherry)sh260* at 3dpf with no overlap of *arg2:GFP* expression in ionocytes with magenta neutrophils.

Figure 2

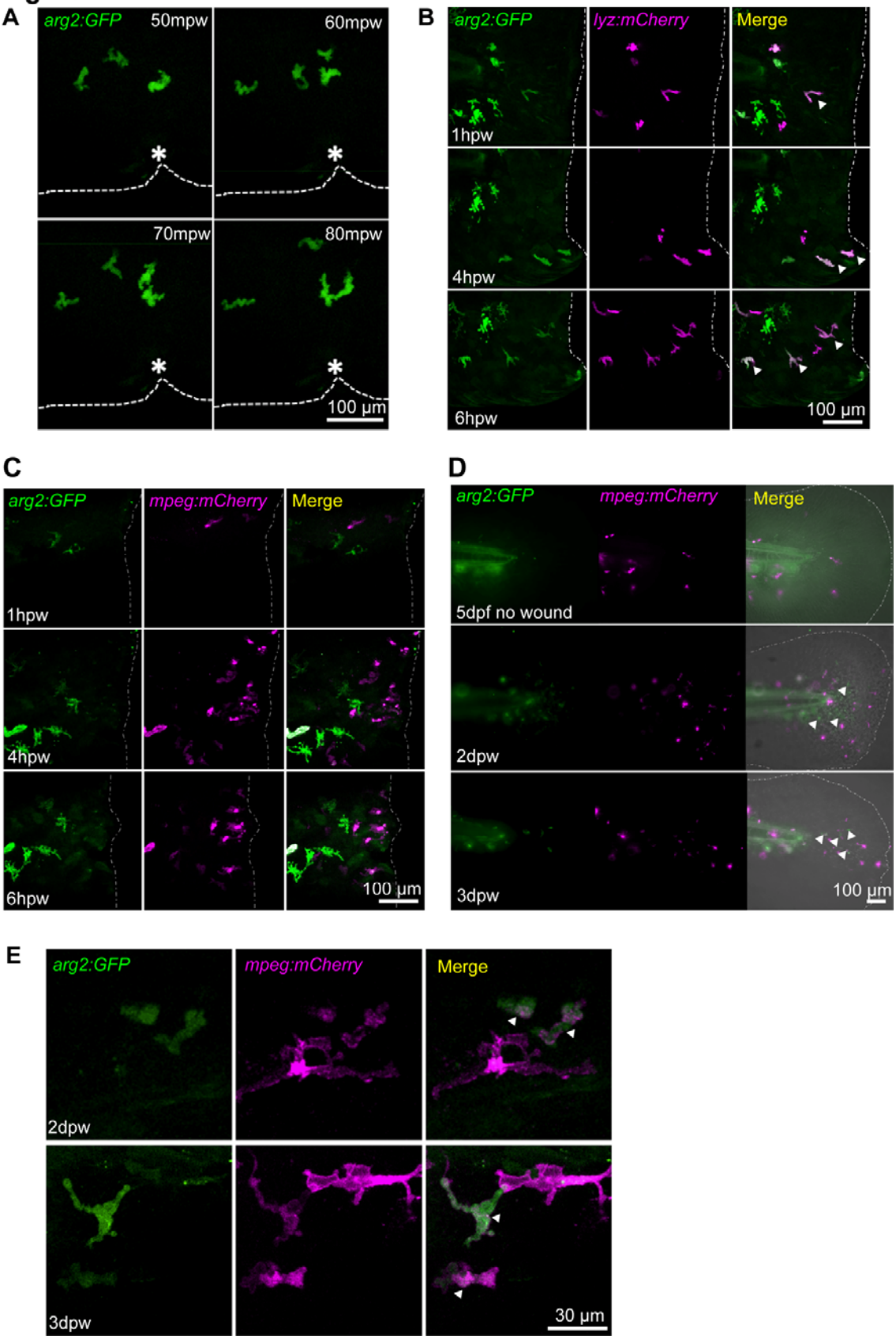

Figure 2: Neutrophils express *arg2:GFP* after wound challenge

(A) Fluorescence confocal timelapse micrographs of *TgBAC(arg2:eGFP)sh571* positive cells migrating towards a tailfin nick wound at early timepoints post injury. Dashed line indicates the edge of the fin and the asterisk marks the nick wound.

(B) Fluorescence confocal micrographs of *arg2:GFP* crossed to *Tg(lyz:nfsB.mCherry)sh260* showing overlap of *arg2:GFP* with neutrophils at a tailfin wound (dashed line). Arrowheads indicate *arg2:GFP* positive neutrophils migrating at the wound.

(C) Fluorescence confocal timelapse micrographs of *arg2:GFP* crossed to *Tg(mpeg1:mCherry)sh378* showing no overlap of macrophages with *arg2:GFP* expression early after injury (dashed line indicates the wound).

(D) Fluorescence widefield micrographs of *arg2:GFP* crossed to *Tg(mpeg1:mCherry)sh378*. The upper panels show an uninjured tailfin with few macrophages and no immune cell *arg2:GFP* expression at 5dpf. The middle panels show an injured tailfin at 2dpw (4dpf) showing no overlap between *mpeg:mCherry* and *arg2:GFP*, but some unlabelled cells expressing *arg2:GFP* with amoeboid, immune cell shape (white arrowheads). Dotted line indicates the edge of the tailfin fold. The lower panels show an injured tailfin at 3dpw (5dpf) showing no overlap between *mpeg:mCherry* and *arg2:GFP*, but some unlabelled cells expressing *arg2:GFP* with amoeboid, immune cell shape (white arrowheads). Dotted line indicates the edge of the tailfin fold.

(E) Fluorescence confocal micrographs of *arg2:GFP* crossed to *Tg(mpeg1:mCherry)sh378* at 2dpw (upper panels) and 3dpw (lower panels), showing examples of *mpeg:mCherry* positive *arg2:GFP* expressing cells in the proximity of the healing wound (arrowheads).

Figure 3

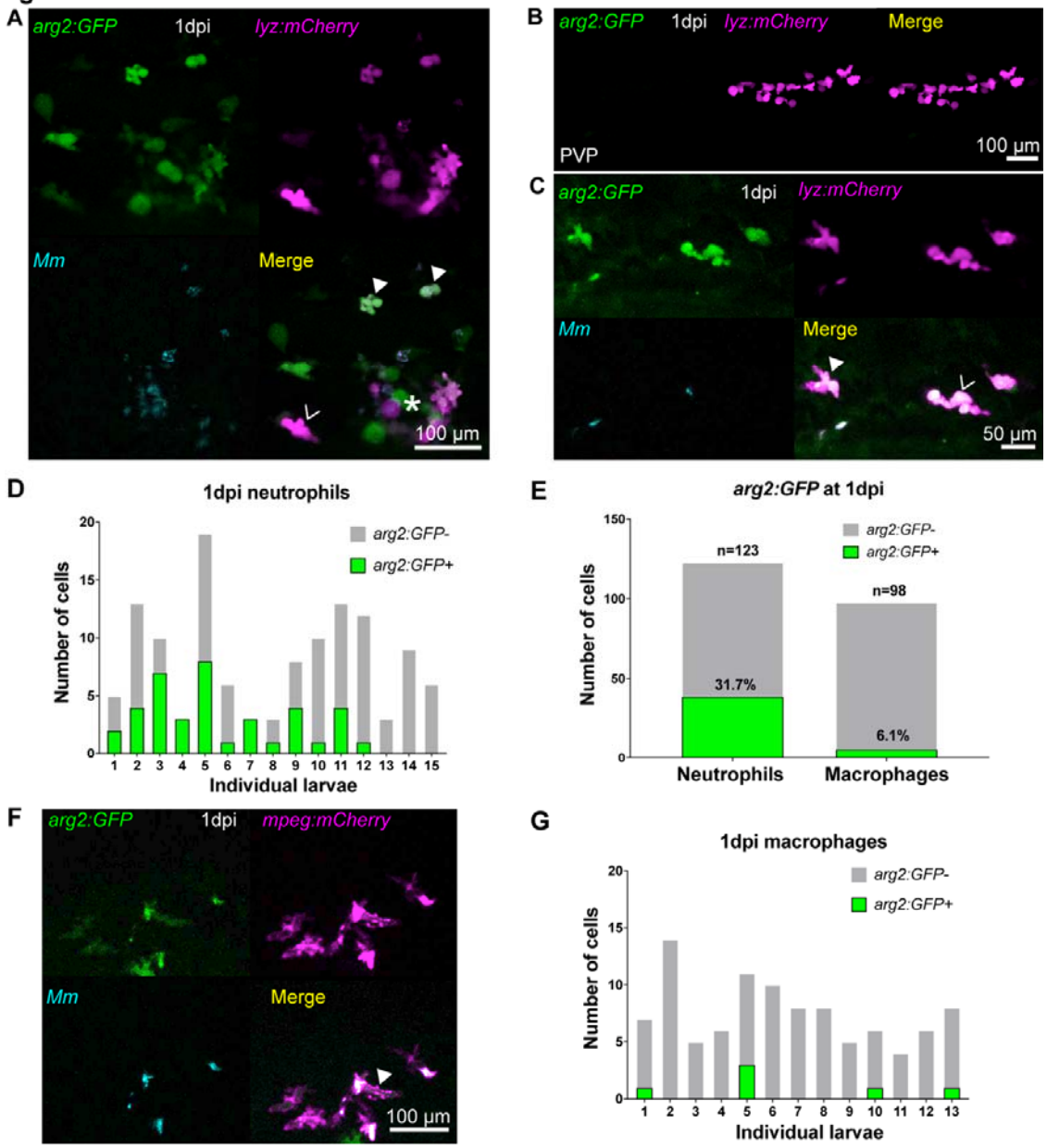

Figure 3: Neutrophils are the predominant immune cell that express *arg2:GFP* post Mm challenge

(A) Fluorescence confocal micrographs of *TgBAC(arg2:GFP)sh571* crossed to *Tg(lyz:nfsB.mCherry)sh260* after Mm infection at 1dpi showing GFP positive neutrophils (filled arrowheads) and GFP negative neutrophils (hollow arrowheads), around an area of high infection (asterisk).

(B) Fluorescence confocal micrographs of 1dpi *arg2:GFP* crossed to *lyz:mCherry* after PVP control injection.

(C) Fluorescence confocal micrographs of *arg2:GFP* crossed to *lyz:mCherry* after Mm infection at 1dpi showing that both infected (filled arrowhead) and non-infected (hollow arrowhead) neutrophils can express *arg2:GFP*.

(D) Graph showing the number of *arg2:GFP* positive and negative neutrophils in a 40x region of interest in the caudal vein region that contained Mm bacteria, post infection, in individual larvae.

(E) Graph showing the percentage of *arg2:GFP* positive and negative neutrophils and macrophages in a 40x region of interest around the infected caudal vein region. Data shown are n = 98-123 cells accumulated over 3 independent experiments.

(F) Fluorescence confocal micrographs of *arg2:GFP* crossed to *Tg(mpeg1:mCherry)sh378* after Mm infection at 1dpi showing a single GFP positive macrophage (filled arrowhead) in this field of view. One of 6 instances observed.

(G) Graph showing the number of *arg2:GFP* positive and negative macrophages in a 40x region of interest in the caudal vein region that contained Mm bacteria post infection in individual larvae.

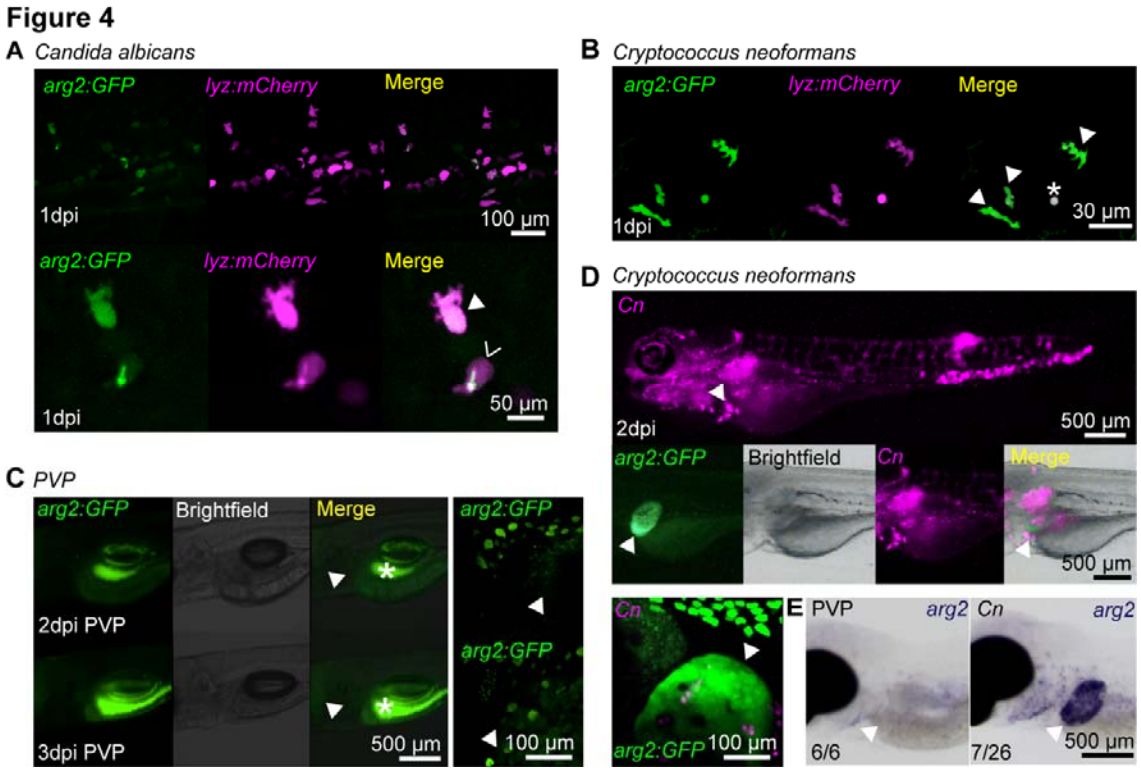

Figure 4: Fungal infections upregulate *arg2:GFP* in neutrophils and the liver

(A) Fluorescence confocal micrographs of *arg2:GFP* crossed to *lyz:mCherry* after *Candida albicans* infection at 1dpi showing GFP positive neutrophils (filled arrowhead) and GFP negative neutrophils (hollow arrowhead), with a zoomed in panel below showing a positive non-infected neutrophil and a GFP negative infected neutrophil (GFP in this cell is autofluorescence from the Candida, which in this instance has survived and formed a hyphae).

(B) Fluorescence confocal micrographs of *arg2:GFP* crossed to *lyz:mCherry* after *Cryptococcus neoformans* infection at 1dpi showing GFP positive neutrophils (filled arrowheads). Asterisk indicates a Cryptococci that is auto fluorescent in both channels.

(C) Brightfield and fluorescence micrographs of *arg2:GFP* larvae at 2dpi and 3dpi after PVP injection. The position of the *arg2:GFP* negative liver is shown by the arrowhead. The GFP channel is turned up highly enough to show gut fluorescence (asterisk) in order to show that the liver is *arg2:GFP* negative.

542 (D) Brightfield and fluorescence micrographs of *arg2:GFP* larvae at 2dpi after *Cryptococcus*
543 *neoformans* (Cn) infection showing *arg2:GFP* liver expression with heavy levels of infection.
544 (E) Brightfield stereo micrographs of *arg2* wholemount *in situ* hybridisation after PVP or
545 *Cryptococcus neoformans* (Cn) infection showing *arg2* liver expression (arrowhead) in an
546 infected individual, not present in the PVP injected larvae.
547

Figure 5

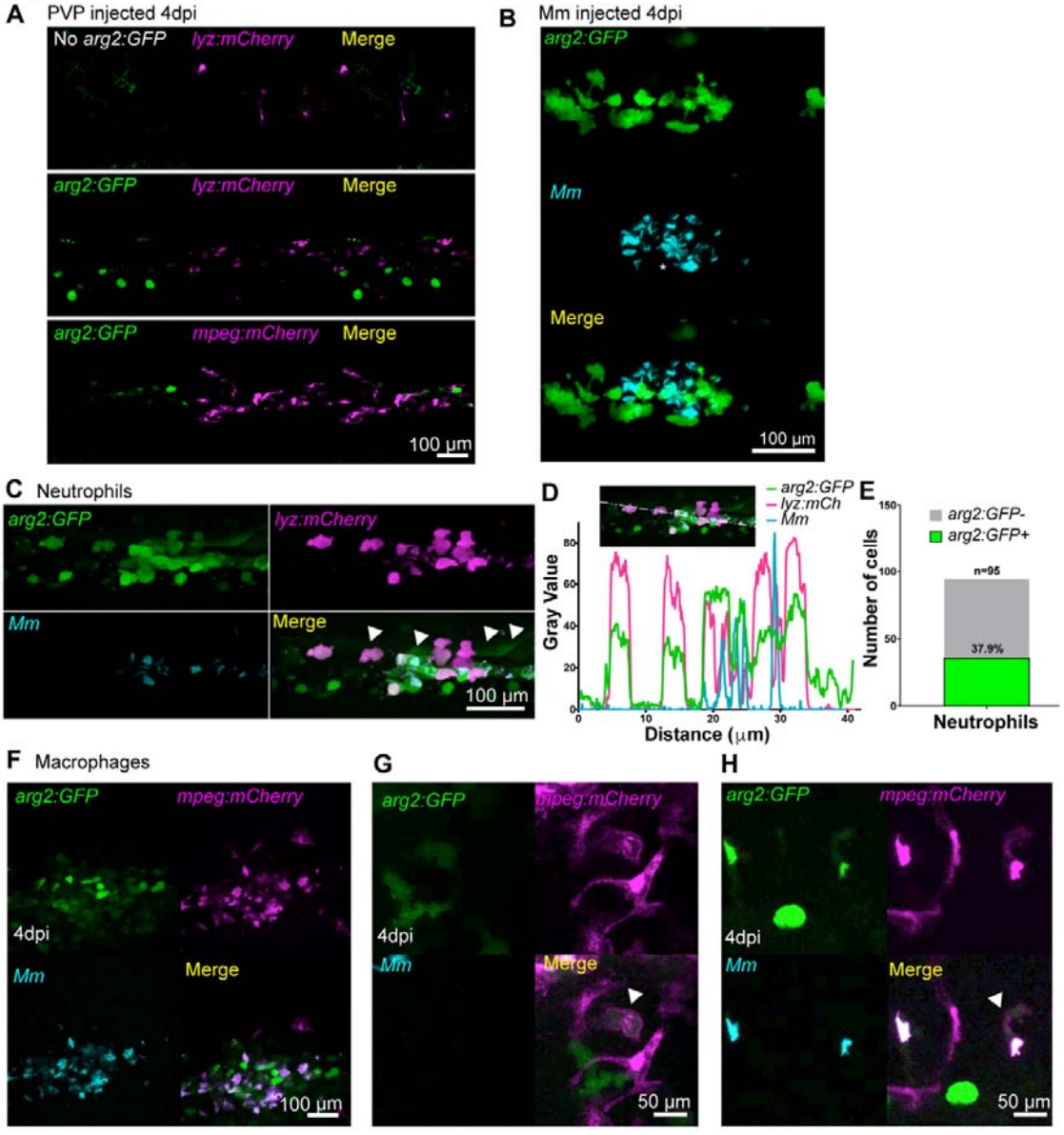

548

549 **Figure 5: A subset of granuloma associated neutrophils and macrophages express**
550 ***arg2:GFP***

551 (A) Fluorescence confocal micrographs of *TgBAC(arg2:GFP)sh571* crossed to
552 *Tg(lyz:nfsB.mCherry)sh260* and *Tg(mpeg1:mCherry)sh378* after PVP control injection at
553 4dpi. Only ionocyte expression of *arg2:GFP* is present.
554 (B) Fluorescence confocal micrographs of *TgBAC(arg2:GFP)sh571* after Mm infection at
555 4dpi showing granuloma associated *arg2:GFP* positive cells.
556 (C) Fluorescence confocal micrographs of *arg2:GFP* crossed to *Tg(lyz:nfsB.mCherry)sh260*
557 after Mm infection at 4dpi, showing neutrophils positive with *arg2:GFP* (filled arrowheads).
558 (D) Line analysis of a cross section through a granuloma showing fluorescence values of
559 *arg2:GFP*, *lyz:GFP* and *Mm*.
560 (E) Graph showing the percentage of *arg2:GFP* positive and negative granuloma-associated
561 neutrophils. Data shown are n = 95 cells accumulated over 3 independent experiments.
562 (F) Fluorescence confocal micrographs of *TgBAC(arg2:GFP)sh571* crossed to
563 *Tg(mpeg1:mCherry)sh378* after Mm infection at 4dpi.
564 (G) Fluorescence confocal micrographs of *arg2:GFP* crossed to *mpeg:mCherry* after Mm
565 infection at 4dpi showing a non-infected, *arg2:GFP* positive macrophage (filled arrowhead).
566 (H) Fluorescence confocal micrographs of *arg2:GFP* crossed to *mpeg:mCherry* after Mm
567 infection at 4dpi showing an infected, *arg2:GFP* positive macrophage (filled arrowhead).
568

569 **Acknowledgements**

570 The authors would like to thank The BSU Aquarium Team for fish care and the IICD
571 Technical Team for practical assistance (University of Sheffield). We would like to
572 thank the Renshaw and Johnston groups for sharing their expertise in BAC
573 transgenesis, especially Miss Catherine Loynes and Dr Stone Elworthy. Thanks to
574 Dr Simon Johnston and Dr Stella Christou for invaluable help and expertise in fungal

infection models. Thanks to Prof Stephen Renshaw for his helpful comments and discussions on the manuscript.

Funding

AL and PME are funded by a Sir Henry Dale Fellowship jointly funded by the Wellcome Trust and the Royal Society (Grant Number 105570/Z/14/A) held by PME. FRH is funded by a University of Sheffield PhD scholarship. Lightsheet imaging was carried out in the Wolfson Light Microscopy Facility, supported by a BBSRC ALERT14 award for light-sheet microscopy (BB/M012522/1).

Author Contributions

Conceived and designed the experiments: FRH, AHM, GFW, PME. Performed the experiments: FRH, AL, HEA, LGW, PME. Generation of *TgBAC(arg2:eGFP)sh571* transgenic zebrafish: AL. Analysed the data: FRH, AL, PME. Wrote and drafted the manuscript: FRH, AL, AHM, GFW, and PME.

Conflicts of Interests

The authors declare that they have no conflicts of interest.

References

1 Hartenstein V (2006) Blood cells and blood cell development in the animal kingdom. *Annu Rev Cell Dev Biol* **22**, 677–712.

2 Duffin R, Leitch AE, Fox S, Haslett C & Rossi AG (2010) Targeting granulocyte apoptosis: mechanisms, models, and therapies. *Immunol Rev* **236**, 28–40.

599 3 Mathias JR, Perrin BJ, Liu T-X, Kanki J, Look AT & Huttenlocher A (2006) Resolution of
600 inflammation by retrograde chemotaxis of neutrophils in transgenic zebrafish. *J*
601 *Leukoc Biol* **80**, 1281–1288.
602 4 Elks PM, van Eeden FJ, Dixon G, Wang X, Reyes-Aldasoro CC, Ingham PW, Whyte MKB,
603 Walmsley SR & Renshaw SA (2011) Activation of hypoxia-inducible factor-1α (Hif-
604 1α) delays inflammation resolution by reducing neutrophil apoptosis and reverse
605 migration in a zebrafish inflammation model. *Blood* **118**, 712–722.
606 5 Phillipson M & Kubes P (2019) The Healing Power of Neutrophils. *Trends Immunol* **40**,
607 635–647.
608 6 Ballesteros I, Rubio-Ponce A, Genua M, Lusito E, Kwok I, Fernández-Calvo G, Khoyratty
609 TE, van Grinsven E, González-Hernández S, Nicolás-Ávila JÁ, Vicanolo T,
610 Maccataio A, Benguría A, Li JL, Adrover JM, Aroca-Crevillen A, Quintana JA, Martín-
611 Salamanca S, Mayo F, Ascher S, Barbiera G, Soehnlein O, Gunzer M, Ginhoux F,
612 Sánchez-Cabo F, Nistal-Villán E, Schulz C, Dopazo A, Reinhardt C, Udalova IA, Ng
613 LG, Ostuni R & Hidalgo A (2020) Co-option of Neutrophil Fates by Tissue
614 Environments. *Cell*.
615 7 Giese MA, Hind LE & Huttenlocher A (2019) Neutrophil plasticity in the tumor
616 microenvironment. *Blood* **133**, 2159–2167.
617 8 Kato T & Kitagawa S (2006) Regulation of neutrophil functions by proinflammatory
618 cytokines. *Int J Hematol* **84**, 205–209.
619 9 Shapouri-Moghaddam A, Mohammadian S, Vazini H, Taghadosi M, Esmaeili S-A, Mardani
620 F, Seifi B, Mohammadi A, Afshari JT & Sahebkar A (2018) Macrophage plasticity,
621 polarization, and function in health and disease. *J Cell Physiol* **233**, 6425–6440.
622 10 Stuehr DJ & Marletta MA (1985) Mammalian nitrate biosynthesis: mouse macrophages
623 produce nitrite and nitrate in response to Escherichia coli lipopolysaccharide. *Proc*
624 *Natl Acad Sci USA* **82**, 7738–7742.

11 Wiegertjes GF, Wentzel AS, Spaink HP, Elks PM & Fink IR (2016) Polarization of immune responses in fish: The “macrophages first” point of view. *Mol Immunol* **69**, 146–156.

12 Munder M, Mollinedo F, Calafat J, Canchado J, Gil-Lamaignere C, Fuentes JM, Luckner C, Doschko G, Soler G, Eichmann K, Müller F-M, Ho AD, Goerner M & Modolell M (2005) Arginase I is constitutively expressed in human granulocytes and participates in fungicidal activity. *Blood* **105**, 2549–2556.

13 Dowling JK, Afzal R, Gearing LJ, Cervantes-Silva MP, Annett S, Davis GM, De Santi C, Assmann N, Dettmer K, Gough DJ, Bantug GR, Hamid FI, Nally FK, Duffy CP, Gorman AL, Liddicoat AM, Lavelle EC, Hess C, Oefner PJ, Finlay DK, Davey GP, Robson T, Curtis AM, Hertzog PJ, Williams BRG & McCoy CE (2021) Mitochondrial arginase-2 is essential for IL-10 metabolic reprogramming of inflammatory macrophages. *Nat Commun* **12**, 1460.

14 Munder M, Eichmann K & Modolell M (1998) Alternative metabolic states in murine macrophages reflected by the nitric oxide synthase/arginase balance: competitive regulation by CD4+ T cells correlates with Th1/Th2 phenotype. *J Immunol* **160**, 5347–5354.

15 Munder M (2009) Arginase: an emerging key player in the mammalian immune system. *Br J Pharmacol* **158**, 638–651.

16 El Kasmi KC, Qualls JE, Pesce JT, Smith AM, Thompson RW, Henao-Tamayo M, Basaraba RJ, König T, Schleicher U, Koo M-S, Kaplan G, Fitzgerald KA, Tuomanen EI, Orme IM, Kanneganti T-D, Bogdan C, Wynn TA & Murray PJ (2008) Toll-like receptor-induced arginase 1 in macrophages thwarts effective immunity against intracellular pathogens. *Nat Immunol* **9**, 1399–1406.

17 MacMicking J, Xie QW & Nathan C (1997) Nitric oxide and macrophage function. *Annu Rev Immunol* **15**, 323–350.

18 Yoshida N, Frickel E-M & Mostowy S (2017) Macrophage–Microbe Interactions: Lessons from the Zebrafish Model. *Front Immunol* **8**.

653 19 Henry KM, Loynes CA, Whyte MKB & Renshaw SA (2013) Zebrafish as a model for the
654 study of neutrophil biology. *J Leukoc Biol* **94**, 633–642.
655 20 Ellett F, Pase L, Hayman JW, Andrianopoulos A & Lieschke GJ (2011) mpeg1 promoter
656 transgenes direct macrophage-lineage expression in zebrafish. *Blood* **117**, e49-56.
657 21 Renshaw SA, Loynes CA, Trushell DMI, Elworthy S, Ingham PW & Whyte MKB (2006) A
658 transgenic zebrafish model of neutrophilic inflammation. *Blood* **108**, 3976–3978.
659 22 Marjoram L, Alvers A, Deerhake ME, Bagwell J, Mankiewicz J, Cocchiaro JL, Beerman
660 RW, Willer J, Sumigray KD, Katsanis N, Tobin DM, Rawls JF, Goll MG & Bagnat M
661 (2015) Epigenetic control of intestinal barrier function and inflammation in zebrafish.
662 *Proc Natl Acad Sci USA* **112**, 2770–2775.
663 23 Ogryzko NV, Lewis A, Wilson HL, Meijer AH, Renshaw SA & Elks PM (2019) Hif-1α-
664 Induced Expression of Il-1β Protects against Mycobacterial Infection in Zebrafish. *J*
665 *Immunol* **202**, 494–502.
666 24 Bojarczuk A, Miller KA, Hotham R, Lewis A, Ogryzko NV, Kamuyango AA, Frost H,
667 Gibson RH, Stillman E, May RC, Renshaw SA & Johnston SA (2016) Cryptococcus
668 neoformans Intracellular Proliferation and Capsule Size Determines Early
669 Macrophage Control of Infection. *Sci Rep* **6**, 21489.
670 25 Buchan KD, Prajsnar TK, Ogryzko NV, de Jong NWM, van Gent M, Kolata J, Foster SJ,
671 van Strijp JAG & Renshaw SA (2019) A transgenic zebrafish line for in vivo
672 visualisation of neutrophil myeloperoxidase. *PLoS ONE* **14**, e0215592.
673 26 Elks PM, Loynes CA & Renshaw SA (2011) Measuring inflammatory cell migration in the
674 zebrafish. *Methods Mol Biol* **769**, 261–275.
675 27 van der Sar AM, Spaink HP, Zakrzewska A, Bitter W & Meijer AH (2009) Specificity of the
676 zebrafish host transcriptome response to acute and chronic mycobacterial infection
677 and the role of innate and adaptive immune components. *Mol Immunol* **46**, 2317–
678 2332.

679 28 Cui C, Benard EL, Kanwal Z, Stockhammer OW, van der Vaart M, Zakrzewska A, Spaink
680 HP & Meijer AH (2011) Infectious disease modeling and innate immune function in
681 zebrafish embryos. *Methods Cell Biol* **105**, 273–308.
682 29 Benard EL, van der Sar AM, Ellett F, Lieschke GJ, Spaink HP & Meijer AH (2012)
683 Infection of zebrafish embryos with intracellular bacterial pathogens. *J Vis Exp*.
684 30 Seman BG, Moore JL, Scherer AK, Blair BA, Manandhar S, Jones JM & Wheeler RT
685 (2018) Yeast and Filaments Have Specialized, Independent Activities in a Zebrafish
686 Model of Candida albicans Infection. *Infection and Immunity* **86**.
687 31 Gibson RH, Evans RJ, Hotham R, Bojarczuk A, Lewis A, Bielska E, May RC, Elks PM,
688 Renshaw SA & Johnston SA (2018) Mycophenolate mofetil increases susceptibility
689 to opportunistic fungal infection independent of lymphocytes. *bioRxiv*, 131540.
690 32 Thisse C & Thisse B (2008) High-resolution in situ hybridization to whole-mount zebrafish
691 embryos. *Nat Protoc* **3**, 59–69.
692 33 Rath M, Müller I, Kropf P, Closs EI & Munder M (2014) Metabolism via Arginase or Nitric
693 Oxide Synthase: Two Competing Arginine Pathways in Macrophages. *Front Immunol*
694 **5**, 532.
695 34 Wentzel AS, Petit J, van Veen WG, Fink IR, Scheer MH, Piazzon MC, Forlenza M,
696 Spaink HP & Wiegertjes GF (2020) Transcriptome sequencing supports a
697 conservation of macrophage polarization in fish. *Sci Rep* **10**, 13470.
698 35 Wentzel AS, Janssen JJE, de Boer VCJ, van Veen WG, Forlenza M & Wiegertjes GF
699 (2020) Fish Macrophages Show Distinct Metabolic Signatures Upon Polarization.
700 *Front Immunol* **11**.
701 36 Rougeot J, Torraca V, Zakrzewska A, Kanwal Z, Jansen HJ, Sommer F, Spaink HP &
702 Meijer AH (2019) RNAseq Profiling of Leukocyte Populations in Zebrafish Larvae
703 Reveals a cxcl11 Chemokine Gene as a Marker of Macrophage Polarization During
704 Mycobacterial Infection. *Front Immunol* **10**, 832.

705 37 Athanasiadis EI, Botthof JG, Andres H, Ferreira L, Lio P & Cvejic A (2017) Single-cell
706 RNA-sequencing uncovers transcriptional states and fate decisions in
707 haematopoiesis. *Nature Communications* **8**, 2045.
708 38 Hsiao C-D, You M-S, Guh Y-J, Ma M, Jiang Y-J & Hwang P-P (2007) A positive
709 regulatory loop between foxi3a and foxi3b is essential for specification and
710 differentiation of zebrafish epidermal ionocytes. *PLoS ONE* **2**, e302.
711 39 Eisenhoffer GT, Slattum G, Ruiz OE, Otsuna H, Bryan CD, Lopez J, Wagner DS,
712 Bonkowsky JL, Chien C-B, Dorsky RI & Rosenblatt J (2017) A toolbox to study
713 epidermal cell types in zebrafish. *J Cell Sci* **130**, 269–277.
714 40 Jänicke M, Carney TJ & Hammerschmidt M (2007) Foxi3 transcription factors and Notch
715 signaling control the formation of skin ionocytes from epidermal precursors of the
716 zebrafish embryo. *Dev Biol* **307**, 258–271.
717 41 Wagener J, MacCallum DM, Brown GD & Gow NAR (2017) Candida albicans Chitin
718 Increases Arginase-1 Activity in Human Macrophages, with an Impact on
719 Macrophage Antimicrobial Functions. *mBio* **8**.
720 42 Brothers KM & Wheeler RT (2012) Non-invasive imaging of disseminated candidiasis in
721 zebrafish larvae. *J Vis Exp*.
722 43 Wright PA, Campbell A, Morgan RL, Rosenberger AG & Murray BW (2004) Dogmas and
723 controversies in the handling of nitrogenous wastes: Expression of arginase Type I
724 and II genes in rainbow trout: influence of fasting on liver enzyme activity and mRNA
725 levels in juveniles. *Journal of Experimental Biology* **207**, 2033–2042.
726 44 Cronan MR, Hughes EJ, Brewer WJ, Viswanathan G, Hunt EG, Singh B, Mehra S,
727 Oehlers SH, Gregory SG, Kaushal D & Tobin DM (2021) A non-canonical type 2
728 immune response coordinates tuberculous granuloma formation and epithelialization.
729 *Cell* **184**, 1757-1774.e14.
730 45 Nguyen-Chi M, Laplace-Builhe B, Travnickova J, Luz-Crawford P, Tejedor G, Phan QT,
731 Duroux-Richard I, Levraud J-P, Kissa K, Lutfalla G, Jorgensen C & Djouad F (2015)
732 Identification of polarized macrophage subsets in zebrafish. *Elife* **4**, e07288.

733 46 Cicchese JM, Evans S, Hult C, Joslyn LR, Wessler T, Millar JA, Marino S, Cilfone NA,
734 Mattila JT, Linderman JJ & Kirschner DE (2018) Dynamic balance of pro- and anti-
735 inflammatory signals controls disease and limits pathology. *Immunol Rev* **285**, 147–
736 167.
737 47 Elks PM, Brizee S, van der Vaart M, Walmsley SR, van Eeden FJ, Renshaw SA & Meijer
738 AH (2013) Hypoxia inducible factor signaling modulates susceptibility to
739 mycobacterial infection via a nitric oxide dependent mechanism. *PLoS Pathog* **9**,
740 e1003789.
741 48 Abebe T, Takele Y, Weldegebreal T, Cloke T, Closs E, Corset C, Hailu A, Hailu W, Sisay
742 Y, Corware K, Corset M, Modolell M, Munder M, Tacchini-Cottier F, Müller I & Kropf
743 P (2013) Arginase activity - a marker of disease status in patients with visceral
744 leishmaniasis in ethiopia. *PLoS Negl Trop Dis* **7**, e2134.
745 49 Jacobsen LC, Theilgaard-Mönch K, Christensen EI & Borregaard N (2007) Arginase 1 is
746 expressed in myelocytes/metamyelocytes and localized in gelatinase granules of
747 human neutrophils. *Blood* **109**, 3084–3087.
748 50 Oliveira-Brito PKM, Rezende CP, Almeida F, Roque-Barreira MC & da Silva TA (2020)
749 iNOS/Arginase-1 expression in the pulmonary tissue over time during Cryptococcus
750 gattii infection. *Innate Immun* **26**, 117–129.
751 51 Mantovani A, Sica A, Sozzani S, Allavena P, Vecchi A & Locati M (2004) The chemokine
752 system in diverse forms of macrophage activation and polarization. *Trends Immunol*
753 **25**, 677–686.
754 52 Benard EL, Racz PI, Rougeot J, Nezhinsky AE, Verbeek FJ, Spaink HP & Meijer AH
755 (2015) Macrophage-expressed perforins mpeg1 and mpeg1.2 have an anti-bacterial
756 function in zebrafish. *J Innate Immun* **7**, 136–152.
757 53 Berüter J, Colombo JP & Bachmann C (1978) Purification and properties of arginase
758 from human liver and erythrocytes. *Biochem J* **175**, 449–454.

759 54 Haraguchi Y, Takiguchi M, Amaya Y, Kawamoto S, Matsuda I & Mori M (1987) Molecular
760 cloning and nucleotide sequence of cDNA for human liver arginase. *Proc Natl Acad*
761 *Sci U S A* **84**, 412–415.
762 55 Shah VS, Chivukula RR, Lin B, Waghray A & Rajagopal J (2022) Cystic Fibrosis and the
763 Cells of the Airway Epithelium: What Are Ionocytes and What Do They Do? *Annu*
764 *Rev Pathol* **17**, 23–46.
765